ARTICLE

Theoretical Study of Reagent Rotational Excitation Effect on the Stereodynamics of H+LiF→HF+Li Reaction

Ting-xian Xie[a], Ying-ying Zhang[b], Ying Shi[b*], Ming-xing Jin[b]

a. Department of Physics, Dalian Jiaotong University, Dalian 116028, China
b. Institute of Atomic and Molecular Physics, Jilin University, Changchun 130012, China

(Dated: Received on June 9, 2013; Accepted on October 14, 2013)

The reagent rotational excitation effect on the stereodynamics of H+LiF→HF+Li is calculated by means of the quasi-classical trajectory method on the Aguado-Paniagua2-potential energy surface (AP2-PES) constructed by Aguado *et al.* [J. Chem. Phys. **106**, 1013 (1997)]. The angular distributions of vector correlations between products and reactants, $P(\theta_r)$ and $P(\phi_r)$ are presented. Meanwhile, the four polarization-dependent generalized differential cross sections are computed. The results indicate that the reagent rotational quantum numbers have impact on the vector properties of the title reaction. In addition, the reaction probability has been calculated as well.

Key words: Stereodynamics, Quasi-classical trajectory, Polarization-dependent generalized differential cross sections

I. INTRODUCTION

During the past decades, numerous of experimental and theoretical studies for the H+LiF→HF+Li reaction have been reported [1−7] and the reaction has been a prototype of the heavy-heavy-light (HHL) system. Furthermore, the LiHF system has a rather deep van der Waals well in the entrance channel, which causes the long-lived collision complexes and narrow scattering resonances in the energy-dependent reaction probabilities [8]. In the experimental aspects, for example, Loesch *et al.* have reported the crossed molecular beam studies on the Li+HF reaction [9, 10]. Hobel *et al.* have detected the double differential cross sections at different collision energies [11]. Theoretical studies like the exact quantum probabilities for Li+HF and its isotopic variants have been reported by Laganà [12]. In 2012, Li *et al.* have presented the reagent vibration effect for the reaction [13].

Aguado *et al.* constructed a potential energy surface of LiHF system based on 570 MRDCI *ab initio* energy points and carried out wave packet calculations [14]. Later they carried out the fitting of the energy points under the same circumstance [15]. Meanwhile, the three-dimensional time-dependent quantum method was used to investigate the dynamics of the LiHF system [15]. To the best of our knowledge, investigations of experimental and theoretical aspects for its reverse reaction H+LiF→HF+Li have been seldom presented except that Weck *et al.* performed quantum scattering calculations for zero total angular momentum of vibrational excitation effect of the title reaction [8], due to the lack of experimental results with metastable hydrogen atom sources in crossed beams experiments.

In term of the theoretical calculation methods, the *ab initio* calculation has been used to compute the potential energy surface. By means of the *ab initio* calculation, Li *et al.* have carried out the double many-body expansion potential energy surface of NH_3 and NH_2 molecule [16, 17]. Varandas has calculated the *ab initio* potential energy surface of the O+OH reaction [18]. In addition, the quasi-classical trajectory (QCT) method [19−21] has also been widely adopted in the stereodynamics field to calculate a great deal of chemical reactions particularly for the atom-molecule [22−24], the ion-molecule [25−27], and the polyatomic molecules [28−30] reactions which have achieved a great success. Recently, it has been developed by Han and coworkers to propagate trajectories and obtain the stereodynamical quantities with simultaneous treatment [31, 32].

In our present work, in order to gain more dynamical information, we have studied the stereodynamics of the title reaction by using a developed QCT method. Meanwhile, the reagent rotational excitation effect on the vector properties of the reaction is performed and discussed as well.

II. THEORETICAL METHODOLOGY

A. PES and the QCT calculations

The Aguado-Paniagua2-potential energy surface (AP2-PES) given by Aguado *et al.* [15] is employed in the present work. The AP2-PES has a relatively deep

*Author to whom correspondence should be addressed. E-mail: shi_ying@jlu.edu.cn

well in its entrance channel and a nonlinear transition state shifted into the exit channel. The Hamilton's classical equations were integrated numerically in three dimensions. The QCT method [19−21, 33, 34] was also developed. In this work, the collision energy for the title reaction is chosen to be 5.0 kcal/mol. The trajectories are initially installed at an H-LiF internuclear separation of 10 Å, the vibrational and rotational quantum numbers of reactant molecules are taken to be v=0 and j=0−6, respectively. Batches of 5×10^4 trajectories are run for each rotational level and the integration step size of 0.1 fs is used to ensure the conservation of total angular momentum and total energy.

B. Rotational alignment parameter and PDDCSs

In this work, the centre-of-mass (CM) frame is chosen and shown in Fig.1. The z-axis is parallel to the reagent initial relative velocity vector **k**, while the y-axis is perpendicular to the x-z scattering plane which contains the initial and final relative velocity vectors **k** and **k′**. θ_t is the angle between **k′** and **k** which is called the scattering angle. θ_r is the angle between **k** and the rotational angular momentum vector **j′**, and ϕ_r is the dihedral angle of the **k**-**k′**-**j′** correlation. The two angles also refer to the polar angle and the azimuth angle of the vector **j′**, respectively. All of these angles can be derived from the QCT stereodynamical calculations.

The angular distribution function $P(\theta_r)$ which describes the **k**-**j′** correlation can be expanded via the Legendre polynomials, the $P(\phi_r)$ describing the **k**-**k′**-**j′** correlation can be expanded in Fourier series, and the joint probability density function $P(\theta_r, \phi_r)$ can be written as the following [35−41]:

$$P(\theta_r) = \frac{1}{2}\sum_k [k] a_0^k P_k(\cos\theta_r) \tag{1}$$

$$\begin{aligned} a_0^k &= \int_0^\pi P(\theta_r) P_k(\cos\theta_r)\sin\theta_r \mathrm{d}\theta_r \\ &= \langle P_k(\cos\theta_r)\rangle \end{aligned} \tag{2}$$

while k=2 indicates the product rotational alignment

$$a_0^2 = \langle P_2(\cos\theta_r)\rangle = \langle P_2(j'k)\rangle \tag{3}$$

$$\begin{aligned} P(\phi_r) = \frac{1}{2\pi}\Bigg(1 + \sum_{n_{\mathrm{even}}\geq 2} a_n \cos n\phi_r + \\ \sum_{n_{\mathrm{odd}}\geq 1} b_n \sin n\phi_r\Bigg) \end{aligned} \tag{4}$$

$$a_n = 2\langle \cos n\phi_r\rangle, \qquad b_n = 2\langle \sin n\phi_r\rangle \tag{5}$$

$$\begin{aligned} P(\theta_r, \phi_r) &= \frac{1}{4\pi}\sum_{kq}[k]\, a_q^k C_{kq}(\theta_r, \phi_r)^* \\ &= \frac{1}{4\pi}\sum_k\sum_{q\geq 0}(a_{a\pm}^k \cos q\phi_r - \\ &\quad a_{q\mp}^k i \sin q\phi_r) C_{kq}(\theta_r, 0) \end{aligned} \tag{6}$$

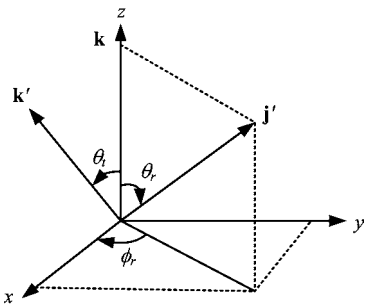

FIG. 1 Centre-of-mass coordinate system used to describe the **k**, **k′**, and **j′** correlations.

The value of the polarization parameter is evaluated as follows:

$$a_q^k = \begin{cases} 2\langle C_{k|q|}(\theta_r, 0)\cos q\phi_r\rangle, & k = \text{even} \\ 2\langle C_{k|q|}(\theta_r, 0)\sin q\phi_r\rangle, & k = \text{odd} \end{cases} \tag{7}$$

In our calculations, the $P(\theta_r, \phi_r)$ is expanded up to k=7, which is sufficient for good convergence. Details on the dynamical information of $P(\theta_r)$, $P(\phi_r)$, and $P(\theta_r, \phi_r)$ are discussed later.

The full three-dimensional angular distribution associated with **k**-**k′**-**j′** correlation can be represented by a set of PDDCSs in the CM frame. The fully correlated CM angular distribution is written as [42−45]:

$$P(\omega_t, \omega_r) = \sum_{kq}\frac{[k]}{4\pi}\frac{1}{\sigma}\frac{\mathrm{d}\sigma_{kq}}{\mathrm{d}\omega_t} C_{kq}(\theta_r, \phi_r)^* \tag{8}$$

$$\frac{1}{\sigma}\frac{\mathrm{d}\sigma_{kq\pm}}{\mathrm{d}\omega_t} = \sum_{k_1}\frac{[k_1]}{4\pi} S_{kq\pm}^{k_1} C_{k_1-q}(\theta_T, 0) \tag{9}$$

$$S_{kq\pm}^{k_1} = \langle c_{k_1 q}(\theta_t, 0) c_{kq}(\theta_r, 0)[(-1)^q e^{iq\phi_r} \pm e^{-iq\phi_r}]\rangle \tag{10}$$

The $\dfrac{1}{\sigma}\dfrac{\mathrm{d}\sigma_{kq\pm}}{\mathrm{d}\omega_t}$ is the polarization-dependent generalized differential cross section (PDDCS), and the angular brackets represent an average over all the reactive trajectories. The PDDCS with q=0 is given by

$$\frac{1}{\sigma}\frac{\mathrm{d}\sigma_{00}}{\mathrm{d}\omega_t} = \frac{1}{4\pi}\sum_{k_1}[k_1] S_{k_0}^{k_1} P_{k_1}(\cos\theta_t) \tag{11}$$

$$S_{k_0}^{k_1} = \langle P_{k_1}(\cos\theta_t) P_k(\cos\theta_t)\rangle \tag{12}$$

Many photon-initiated bimolecular reaction experiments will be sensitive to only those polarization moments with k=0 and 2. In this work, the four PDDCSs, $(2\pi/\sigma)(\mathrm{d}\sigma_{00}/\mathrm{d}\omega_t)$, $(2\pi/\sigma)(\mathrm{d}\sigma_{20}\mathrm{d}\omega_t)$, $(2\pi/\sigma)(\mathrm{d}\sigma_{22^+}/\mathrm{d}\omega_t)$, and $(2\pi/\sigma)(\mathrm{d}\sigma_{22^-}/\mathrm{d}\omega_t)$ are calculated.

III. RESULTS AND DISCUSSION

In our calculations, we plot all the vector correlation functions and the PDDCSs in three dimensions.

DOI:10.1063/1674-0068/27/01/39-44

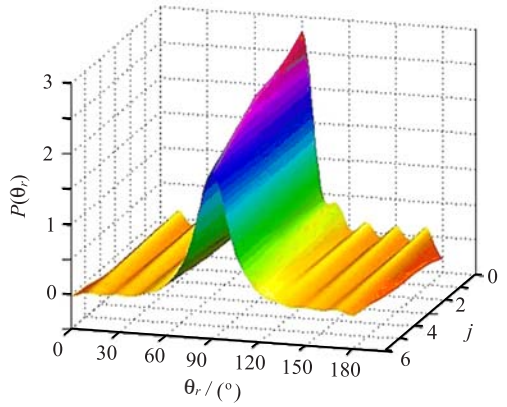

FIG. 2 Distributions of $P(\theta_r)$ reflecting $\mathbf{k}$-$\mathbf{j}'$ correlations at different rotational levels j=0−6 for the title reaction.

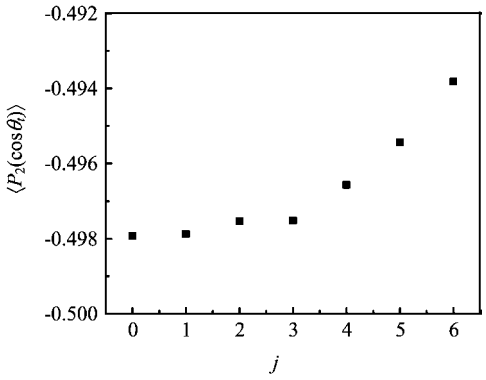

FIG. 3 Variation of rotational alignment parameter $\langle P_2(\cos\theta_r)\rangle$ with rotational levels j=0 to j=6 for the title reaction.

Figure 2 illustrates the product angular distributions $P(\theta_r)$ describing the $\mathbf{k}$-$\mathbf{j}'$ correlation. The peaks are situated at θ_r=90° and also symmetric with respect to θ_r=90° at all calculated rotational levels, which reveal that the product rotational angular momentum vector $\mathbf{j}'$ is strongly aligned along the direction perpendicular to the direction of the reagent relative velocity $\mathbf{k}$. Furthermore, the values of the peaks become lower and broader as the rotational level increases, indicating that influence of the product alignment becomes weaker at high rotational levels. The result can be reflected via the rotational alignment parameter $\langle P_2(\cos\theta_r)\rangle$ depicted in Fig.3. We can obtain that with increasing of the rotational level, the negative values of the $\langle P_2(\cos\theta_r)\rangle$ become smaller which indicates a weaker alignment as well.

Figure 4 demonstrates the dihedral angle distributions $P(\phi_r)$ which represent the $\mathbf{k}$-$\mathbf{k}'$-$\mathbf{j}'$ correlation. From inside to the outside, the corresponding rotational state is j=0, j=3, and j=6, respectively. The incremental direction of ϕ_r moves clockwise. It shows that the distributions of $P(\phi_r)$ are asymmetric with ϕ_r=180° at all the rotational states which indicates a strong polar-

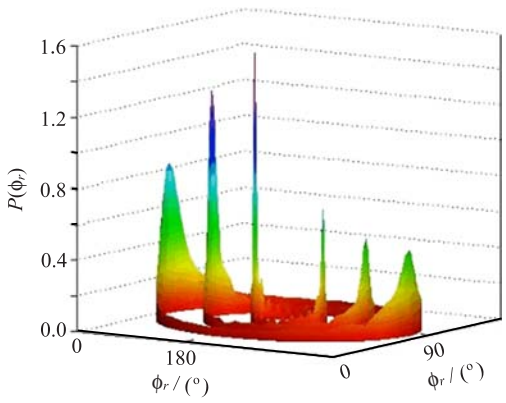

FIG. 4 Dihedral angle distribution of $P(\phi_r)$ with respect to the $\mathbf{k}$-$\mathbf{k}'$ plane, plotted at reagent rotational quantum numbers j=0, j=3, and j=6, respectively.

ization of the angular momentum. The two major peaks are at ϕ_r=90° and ϕ_r=270°. Obviously, the peaks at ϕ_r=270° are far stronger than the peaks at ϕ_r=90°, which reflects that $\mathbf{j}'$ is not only aligned along the y axis but also oriented along the negative direction of the y-axis in the CM frame. This appearance of the result can be explained by the impulse model [37] about the A+BC→AB+C reaction [46−48]. The product angular momentum vector $\mathbf{j}'$ is given by

$$\mathbf{j}' = L\sin^2\beta + j\cos^2\beta + \frac{J_1 m_{\rm A}}{m_{\rm B}} \tag{13}$$

$$J_1 = (\mu_{\rm BC}R)^{1/2}(\mathbf{r}_{\rm AB}\times\mathbf{r}_{\rm CB}) \tag{14}$$

where L is the reagent orbital angular momentum, $\mathbf{r}_{\rm AB}$ and $\mathbf{r}_{\rm CB}$ are unit vectors. $\mu_{\rm BC}$ is the reduced mass of molecule BC and R is the repulsive energy. The term J_1 plays a vital role in the product rotational orientation. The $L\sin^2\beta + j\cos^2\beta$ is symmetric, while for the effect of R, the term $J_1 m_{\rm A}/m_{\rm B}$ shows a prioritized direction which leads to the left-handed HF product rotation in plane parallel to the $\mathbf{k}$-$\mathbf{k}'$ scattering plane.

In order to obtain more stereodynamical information on the effect of rotational quantum numbers and have a better observation of the product angular momentum polarization which reflects the $\mathbf{k}$-$\mathbf{k}'$-$\mathbf{j}'$ correlation, the distributions of $P(\theta_r,\phi_r)$ are depicted in Fig.5. In this work, we only show the distributions at rotational quantum numbers j=0, j=3, and j=6. The two peaks at (90°,90°) and (90°,270°) are in good agreement with the distributions of $P(\theta_r)$ and $P(\phi_r)$ mentioned above. Meanwhile, the plot of the distributions indicates that the HF products are preferentially polarized perpendicular to the scattering plane and the reaction is dominated by in-plane mechanisms [49].

The PDDCSs describing the $\mathbf{k}$-$\mathbf{k}'$-$\mathbf{j}'$ correlation and the scattering direction of the HF product molecule have been displayed in Fig.6. In our present work, the four PDDCSs, $(2\pi/\sigma)(\mathrm{d}\sigma_{00}/\mathrm{d}\omega_t)$, $(2\pi/\sigma)(\mathrm{d}\sigma_{20}\mathrm{d}\omega_t)$, $(2\pi/\sigma)(\mathrm{d}\sigma_{22^+}\mathrm{d}\omega_t)$, and $(2\pi/\sigma)(\mathrm{d}\sigma_{22^-}\mathrm{d}\omega_t)$ are com-

DOI:10.1063/1674-0068/27/01/39-44

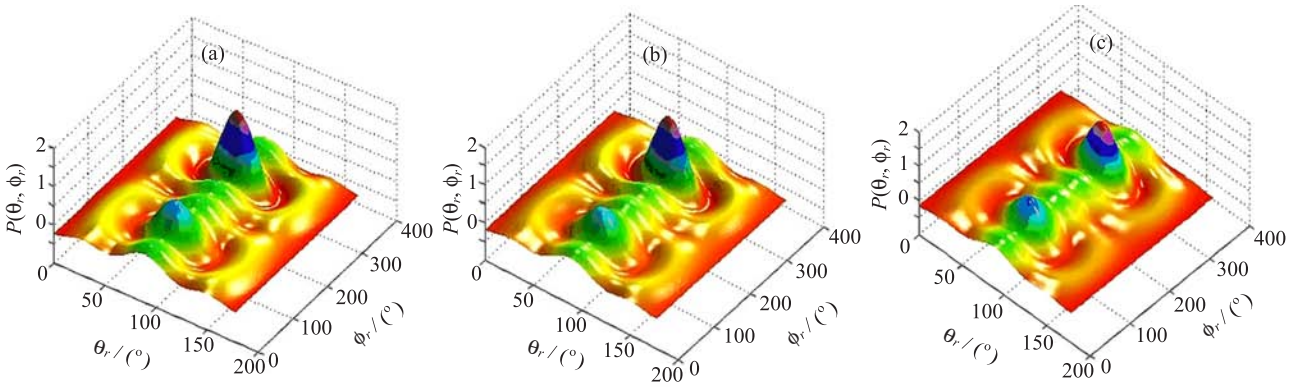

FIG. 5 Polar plots of the $P(\theta_r, \phi_r)$ distributions with peaks and valleys at different rotational states. (a) j=0, (b) j=3, and (c) j=6.

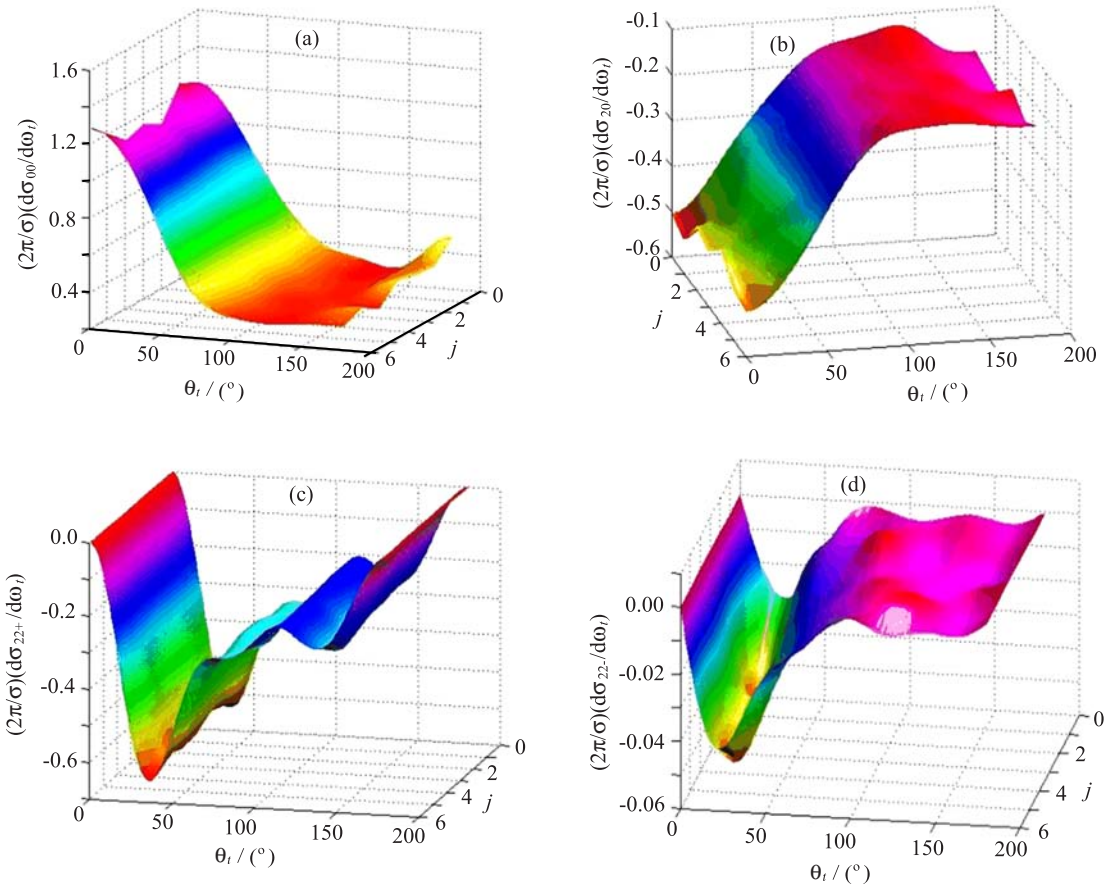

FIG. 6 Four PDDCSs of the reagent rotational quantum numbers with (a) (k,q)=(0,0), (b) (k,q)=(2,0), (c) (k,q)=(2,2^+), and (d) (k,q)=(2,1^-), respectively.

puted at all rotational levels from j=0 to j=5. The PDDCS $(2\pi/\sigma)(d\sigma_{00}d\omega_t)$ which only describes the **k**-**k**′ correlation or the scattering direction of the product is a simple differential cross section and has no ties to the orientation and alignment of the product rotational angular momentum vector **j**′. As shown in Fig.6(a), with increasing of the rotational quantum numbers, the forward scattering of product HF becomes weaker while the backward scattering turns stronger. The PDDCS $(2\pi/\sigma)(d\sigma_{20}/d\omega_t)$ which shows an opposite trend to the PDDCS $(2\pi/\sigma)(d\sigma_{00}/d\omega_t)$ is the expectation value of the second Legendre moment drawn in Fig.6(b). Clearly, the values of PDDCS $(2\pi/\sigma)(d\sigma_{20}/d\omega_t)$ are negative which is probably associated with the alignment moment $\langle P_2(\cos\theta_r)\rangle$.

The PDDCSs with $q\neq0$ are shown in Fig.6 (c) and

DOI:10.1063/1674-0068/27/01/39-44

TABLE I Reaction probability as a function of the impact parameter at rotational level j=0 to j=6.

b	j=0	j=1	j=2	j=3	j=4	j=5	j=6
0	0.01944	0.0144	0.0184	0.0162	0.0135	0.0152	0.0243
1	0.0179	0.017	0.0178	0.0186	0.0166	0.0169	0.0253
2	0.0186	0.0169	0.0141	0.0169	0.0142	0.0161	0.0245
3	0.0186	0.0209	0.0187	0.0198	0.0214	0.02	0.0252
4	0.021	0.0205	0.0206	0.0191	0.0196	0.0199	0.0206
5	0.022	0.0208	0.0226	0.0171	0.0149	0.0107	0.0122
6	0.0187	0.0197	0.0146	0.0122	0.0106	0.0106	0.0096
7	0.0148	0.0132	0.0108	0.0082	0.007	0.006	0.0069

(d). In some manners, the distributions of the PDDCSs with $q\neq0$ are necessarily zero at the extremely forward and backward scattering. Figure 6(c) illustrates the distributions of PDDCS $(2\pi/\sigma)(\mathrm{d}\sigma_{22^+}/\mathrm{d}\omega_t)$. We can obtain that the values of the distributions are negative at all scattering angles which correspond to the product rotational alignment that shows a preference along the y-axis. There are two stronger polarizations ranging from 35°−40° and 136°−141°, respectively. In addition, it also reflects that the product angular momentum distribution is anisotropic. The PDDCS $(2\pi/\sigma)(\mathrm{d}\sigma_{21^-}/\mathrm{d}\omega_t)$ reflects the product rotational angular momentum vector $\mathbf{j}'$ is along the direction of vector $x-z$ or $x+z$. Figure 6(d) displays a strong negative peaks ranging from 21° to 26° which indicates the rotational alignment of the HF products is along the $x+z$ direction. Moreover, the distributions of $(2\pi/\sigma)(\mathrm{d}\sigma_{21^-}/\mathrm{d}\omega_t)$ are all in such small values which implie that the product angular momentum distribution is isotropic.

In order to obtain more about the title reaction, the rotational excitation effect of its scalar properties is computed as well. Table I displays the reaction probability as a function of the impact parameter with the rotational quantum numbers ranging from j=0 to j=6. Generally speaking, the values of the reaction probability are small and change little at all rotational levels and impact parameters which means that the reaction probability doesn't strongly depend on the rotational levels. The similar phenomenon has also been observed in reactions like H+O_2 [50−52], O+H_2 [53] and other reactions [54, 55] which may attribute to the deep well on the potential energy surface in this type of reactions.

IV. CONCLUSION

Investigations on the stereodynamics of the H+LiF→HF+Li reaction have been performed by the QCT method on the AP2-PES at rotational levels from j=0 to j=6. The collision energy for the title reaction is taken to be 5.0 kcal/mol. We have studied the angular distributions of $P(\theta_r)$ and $P(\phi_r)$. The distributions of $P(\theta_r)$ reveals a strong product rotational alignment and the distribution $P(\phi_r)$ shows a asymmetric behavior to the scattering plane and exhibits two peaks at ϕ_r=90° and ϕ_r=270° and peaks at ϕ_r=270° are stronger than those at ϕ_r=90° which can be explained by the implosive model which implies that $\mathbf{j}'$ is not only aligned but also oriented along the negative direction of the y-axis. In addition, we have calculated the four PDDCSs. The PDDCS $(2\pi/\sigma)(\mathrm{d}\sigma_{00}/\mathrm{d}\omega_t)$ shows a weakly forward scattering and strongly backward scattering of the product HF with the increase of the rotational states. The PDDCS $(2\pi/\sigma)(\mathrm{d}\sigma_{20}/\mathrm{d}\omega_t)$ indicates that $\mathbf{j}'$ is strongly aligned the direction perpendicular to k. The PDDCS $(2\pi/\sigma)(\mathrm{d}\sigma_{22^+}/\mathrm{d}\omega_t)$ reveals that the product angular momentum distribution is anisotropic while the PDDCS $(2\pi/\sigma)(\mathrm{d}\sigma_{21^-}/\mathrm{d}\omega_t)$ reflects its isotropy. Finally, the reaction probability indicates that the influence of the deep well on the potential energy surface to the initial rotational states of the reagent molecule can't also be ignored.

V. ACKNOWLEDGMENTS

This work was supported by the Jilin University, China (No.419080106440), the Chinese National Fusion Project for ITER (No.2010GB104003), and the National Natural Science Foundation of China (No.10974069). Many thanks to Prof. Ke-li Han for providing the stereodynamics program.

[1] T. J. Odiorne, P. R. Brooks, and J. V. V. Kasper, J. Chem. Phys. **551**, 980 (1971).
[2] Z. Karny, R. C. Estler, and R. N. Zare, J. Chem. Phys. **69**, 5199 (1978).
[3] F. E. Bartoszek, B. A. Blackwell, J. C. Polanyi, and J. J. Sloan, J. Chem. Phys. **74**, 3400 (1981).
[4] M. Baer, I. Last, and H. J. Loesch, J. Chem. Phys. **101**, 9648 (1994).
[5] D. R. Herschbach, Adv. Chem. Phys. **10**, 319 (1996).

DOI:10.1063/1674-0068/27/01/39-44

[6] F. J. Aoiz, E. Verdasco, R. V. Sáez, H. J. Loesch, M. Menéndez, and F. Stienkemeier, Phys. Chem. Chem. Phys. **2**, 541 (2000).
[7] R. S. Tan, X. G. Liu, and M. Hu, Chin. Phys. Lett. **29**, 123101 (2012).
[8] P. F. Weck and N. Balakrishnan, J. Chem. Phys. **122**, 234310 (2005).
[9] H. J. Loesch, S. Stenzel, and B. Wüstenbecker, J. Chem. Phys. **95**, 38419 (1991).
[10] H. J. Loesch and F. Stienkemeier, J. Chem. Phys. **99**, 9598 (1993).
[11] O. Hobel, A. Paladini, A. Russo, R. Bobbenkamp, and H. J. Loesch, Phys. Chem. Chem. Phys. **62**, 198 (2004).
[12] A. Laganà, A. Bolloni, and S. Crocchianti, Phys. Chem. Chem. Phys. **2**, 535 (2000).
[13] S. J. Li, Y. Shi, T. X. Xie, and M. X. Jin, Chin. Phys. B **21**, 013401 (2012).
[14] A. Aguado, C. Sufirez, and M. Paniagua, Chem. Phys. **201**, 107 (1995).
[15] A. Aguado and M. Paniagua, J. Chem. Phys. **106**, 1013 (1997).
[16] Y. Q. Li, Y. Z. Song, P. Song, Y. Z. Li, Y. Ding, M. T. Su, and F. C. Ma, J. Chem. Phys. **136**, 194705 (2012).
[17] Y. Q. Li, J. C. Yuan, M. D. Chen, F. C. Ma, and M. T. Sun, J. Comp. Chem. **34**, 1686 (2013).
[18] A. J. C. Varandas, J. Chem. Phys. **138**, 134117 (2013).
[19] F. J. Aoiz, M. T. Martınez, M. Menéndez, R. V. Sáez, and E. Verdasco, Chem. Phys. Lett. **299**, 25 (1999).
[20] T. G. Yang, J. C. Yuan, D. H. Cheng, and M. D. Chen, Commun. Comput. Chem. **1**, 15 (2013).
[21] M. L. Wang, K. L. Han, J. P. Zhan, V. W. K. Wu, G. Z. He, and N. Q. Lou. Chem. Phys. Lett. **278**, 307 (1997).
[22] A. J. Alexander, F. J. Aoiz, M. Brouard, and J. R. Simons. Chem. Phys. Lett. **256**, 561 (1996).
[23] M. D. Chen, K. L. Han, and N. Q. Lou, Chem. Phys. Lett. **357**, 483 (2002).
[24] T. S. Chu, H. Zhang, S. P. Yuan, A. P. Fu, H. Z. Si, F. H.Tian, and Y. B. Duan, J. Chem. Phys. A **113**, 3470 (2009).
[25] L. Yao, H. Y. Zhong, Y. L. Liu, and W. W. Xia, Chem. Phys. **359**, 151 (2009).
[26] X. H. Li, M. S. Wang, I. Pino, C. L. Yang, and L. Z. Ma, Chem. Phys. **11**, 10438 (2009).
[27] N. Bulut, J. F. Castillo, F. J. Aoiz, and L. Bañares, Chem. Phys. **10**, 821 (2008).
[28] A. J. C. Varandas, P. J. S. B. Caridade, Z. H. Zhang, Q. Cui, and K. L. Han, J. Chem. Phys. **125**, 064312 (2006).
[29] D. Troya and E. Garcia-Molina, J. Phys. Chem. A **109**, 3015 (2005).
[30] M. A. Horst, G. C. Schatz, and L. B. Harding, J. Chem. Phys. **105**, 558 (1996).
[31] X. Zhang and K. L. Han, Int. J. Quantum. Chem. **106**, 1815 (2006).
[32] M. D. Chen, K. L. Han, and N. Q. Lou, Chem. Phys. **283**, 463 (2002).
[33] K. L. Han, G. Z. He, and N. Q. Lou, Chin. J. Chem. Phys. **2**, 323 (1989).
[34] Q. Wei, X. Li, and T. Li, Chin. J. Chem. Phys. **22**, 523 (2009).
[35] W. W. Xu, X. G. Liu, S. X. Luan, S. S. Sun, and Q. G. Zhang, Chin. Phys. B **18**, 339 (2009).
[36] M. Brouard, H. M. Lambert, S. P. Rayner, and J. P. Simons, Mol. Phys. **89**, 403 (1996).
[37] M. L. Wang, K. L. Han, and G. Z. He, J. Chem. Phys. **109**, 4463 (1998).
[38] K. L. Han, L. Zhang, D. L. Xu, G. Z. He, and N. Q. Lou, J. Phys. Chem. A **105**, 2956 (2001).
[39] J. Zhang, T. S. Chu, S. L. Dong, S. P. Yuan, A. P. Fu, and Y. B. Duan, Chin. Phys. Lett. **28**, 093403 (2011).
[40] M. H. Ge and Y. J. Zheng, Chem. Phys. **392**, 185 (2012).
[41] C. X. Yao and G. J. Zhao, Can. J. Chem. **91**, 387 (2013).
[42] W. L. Li, M. S. Wang, C. L. Yang, W. W. Liu, C. Sun, and T. Q. Ren, Chem. Phys. **337**, 93 (2007).
[43] F. J. Aoiz, M. Brouard, and P. A. Enriquez, J. Chem. Phys. **105**, 4964 (1996).
[44] M. L. Wang, K. L. Han, and G. Z. He, J. Chem. Phys. **109**, 5446 (1998).
[45] L. Z. Wang, C. L. Yang, J. J. Liang, J. Xiao, and Q. G. Zhang, Chin. J. Chem. Phys. **24**, 686 (2011).
[46] A. Zanchet, O. Roncero, T. González-Lezana, A. Rodríguez-López, A. Aguado, C. Sanz-Sanz, and S. Gómez-Carrasco, J. Phys. Chem. A **113**, 14488 (2009).
[47] K. L. Han, G. Z. He, and N. Q. Lou, J. Chem. Phys. **105**, 8699 (1996).
[48] C. Suarez, A. Aguado, C. Tablero, and M. Paniagua, Int. J. Quantum Chem. **52**, 935 (1994).
[49] M. D. Chen, K. L. Han, and N. Q. Lou, Chem. Phys. Lett. **357**, 483 (2002).
[50] C. Leforestier and W. H. Miller, J. Chem. Phys. **100**, 733 (1993).
[51] R. T. Pack, E. A. Butcher, and G. A. Parker, J. Chem. Phys. **99**, 9310 (1993).
[52] J. Q. Dai and J. Z. H. Zhang, J. Phys. Chem. **100**, 1898 (1996).
[53] T. Peng, D. H. Zhang, J. Z. H. Zhang, and R. Schinke, Chem. Phys. Lett. **248**, 37 (1996).
[54] D. Kuang, T. Y. Chen, W. P. Zhang, N. J. Zhao, and D. J. Wang, Bull. Korean. Chem. Soc. **31**, 2841 (2010).
[55] Q. T. Meng, J. Zhao, Y. Xu, and D. G. Yue, Chem. Phys. **362**, 65 (2009).

DOI:10.1063/1674-0068/27/01/39-44